

Measurement of Total Hemispherical Emissivity Using a Calorimetric Technique

J. Hameury · B. Hay · J. R. Filtz

Published online: 26 July 2007
© Springer Science+Business Media, LLC 2007

Abstract An apparatus has been designed to measure, using a calorimetric technique, the total hemispherical emissivity of opaque solid materials from -20 to 200°C . The originality of the technique is the use of two samples and thermal guard rings in order to ensure one-dimensional heat flow in each sample and to reduce heat-loss corrections. Two temperatures are measured in each sample at two distances from the surface, and the surface temperature of each sample is linearly extrapolated. The mean total hemispherical emissivity of the two samples is calculated using a model that considers the main surfaces radiating in the chamber. Unwanted heat losses are evaluated and corrected. The facility design, model of calculation, evaluation of corrections, and uncertainty assessment are described. The measurement technique was validated by comparison to results from a study using another technique. The expanded uncertainty ($k = 2$) of the total hemispherical emissivity is between ± 0.005 and ± 0.03 .

Keywords Calorimetric technique · Heat-loss corrections · Solid materials · Total hemispherical emissivity · Uncertainty analysis

1 Introduction

As the French standards laboratory for measurement of radiative properties of materials in the infrared spectrum, Laboratoire National de Métrologie et d'Essais (LNE) has

Paper presented at the the Seventeenth European Conference on Thermophysical Properties, September 5–8, 2005, Bratislava, Slovak Republic.

J. Hameury (✉) · B. Hay · J. R. Filtz
Thermophysical Properties Laboratory, Thermal and Optical Division, Bureau National de Métrologie -
Laboratoire National d'Essais, 1 rue Gaston Boissier, Paris 75015, France
e-mail: jacques.hameury@lne.fr

developed and improved instruments to measure the reflectance, the transmittance, and the emissivity of materials in the infrared spectrum. This paper presents an apparatus designed for measuring the total hemispherical emissivity of solid opaque materials in the temperature range from -20 to 200°C . The objectives included an uncertainty of less than ± 0.03 for a material with a high emissivity (higher than 0.8) and a low thermal conductivity (about $1 \text{ W} \cdot \text{m}^{-1} \cdot \text{K}^{-1}$) and an uncertainty of less than ± 0.01 for a material with a low emissivity (lower than 0.1) or a material with a high emissivity and a high thermal conductivity (higher than $20 \text{ W} \cdot \text{m}^{-1} \cdot \text{K}^{-1}$). Another important objective was to quantify accurately the effect of each significant source of uncertainty. To reach those objectives, a steady-state heat-balance method was preferred to a radiometric technique or to a heat balance transient technique.

Radiometric techniques can be used to compare, with a “total” radiometer, the radiation of the sample to the radiation of a blackbody; such a technique is presented in Ref. [1]. Because of the geometrical limitations of the radiometer, the directional total (all wavelengths) emissivity must be measured for many directions from the normal to the surface to the grazing direction [1]. The total hemispherical emissivity is then calculated by geometrical integration over all directions. To reach a low uncertainty, the radiometric comparisons must be made in vacuum to avoid absorption and emission by the atmosphere and to avoid disturbances due to convection [1]. The radiometer must have a constant spectral sensitivity over the spectral range corresponding to the temperature of the sample ($5\text{--}50 \mu\text{m}$ for room temperature). Practically, this specification is not easy to check and the more suitable detectors are thermal detectors that are not very sensitive.

In heat balance transient techniques, the speed of variation of the sample temperature is used to calculate the heat flux density gained or lost by the surface of the sample. Refs. [2–4] describe different transient techniques to measure the total hemispherical emissivity. For those methods, the thermal heat capacity and the thermal diffusivity of the material must be known; for materials with a high thermal conductivity, the heat capacity can be sufficient [2]. Techniques normally used to measure heat capacity (differential scanning calorimetry) and diffusivity (laser flash technique) give relative uncertainties of about 2–5%. Moreover, transient techniques use thermal models, more or less simplified, to calculate the surface temperature and the heat flux density. Hence, the relative uncertainty on the measured total hemispherical emissivity can be relatively large [2]. The technique chosen by LNE is based on existing steady-state heat balance techniques [5–7], with two samples. Two identical samples are heated by an electrical resistor placed between them. The innovation is that the two samples (disc shape) are surrounded by thermal guard rings as in the “guarded hot plate” used to measure the thermal conductivity of insulating materials [8].

2 Description of the Apparatus

The apparatus was designed and built at LNE; Fig. 1 shows a general diagram of the apparatus. The heater, used to heat two identical samples surrounded by a thermal guard, is suspended at the mid-height of a black vacuum chamber thermostatted with boiling nitrogen. A pc controls the measurements of the electrical power supplied to

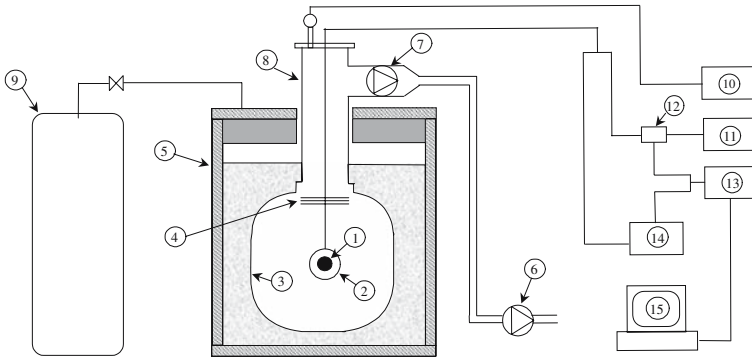


Fig. 1 LNE total hemispherical emissometer: (1) sample; (2) heating system; (3) chamber; (4) radiative screens; (5) Dewar; (6) valve vacuum pump; (7) turbomolecular vacuum pump; (8) access well; (9) nitrogen tank; (10) manometer; (11) electrical supply; (12) calibrated shunt resistor; (13) voltmeter; (14) 0°C reference for thermocouples; (15) computer

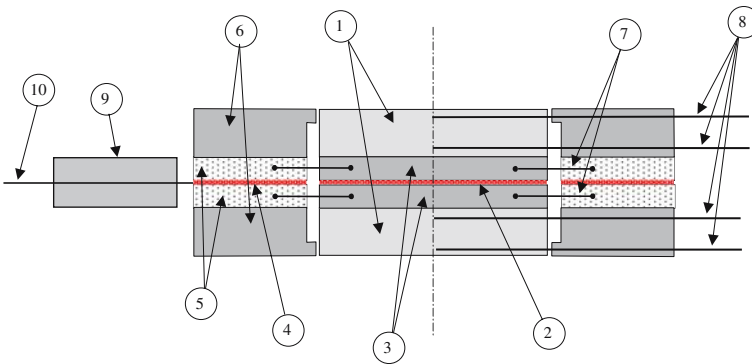


Fig. 2 Cross section of the heating system with samples and rings: (1) samples; (2) sample heating resistor; (3) copper discs; (4) guard-ring heating resistor; (5) copper rings; (6) sample rings; (7) thermopile, (8) thermocouples; (9) wire guard block; (10) wires

the sample heater and the measurements of the temperatures of the samples and the thermal guard. A Eurotherm controller controls the temperatures of the sample heater and the thermal guard. The total hemispherical emissivity is measured on two samples of the same material in order to reduce the ratio of the unwanted heat flux, lost or gained by the system, to the useful heat flux radiated by the samples. The use of two samples is particularly relevant when the emissivity of the material is low so that the heat flux radiated by the samples is low. This arrangement avoids the use of a thermal guard barrier that would be needed to reduce the heat flux lost by the back side of the heating system, if only one sample was used. With the guard rings, it is also possible to use thick samples, which is required by the measurement technique of the surface temperature. The heat flow in each sample is one-dimensional; thus, the mean surface temperature of each sample can be measured more accurately. The guard rings reduce the thermal perturbations in the samples due to heat leakages along the thermocouples; indeed, those thermal perturbations are mainly concentrated in the guard rings.

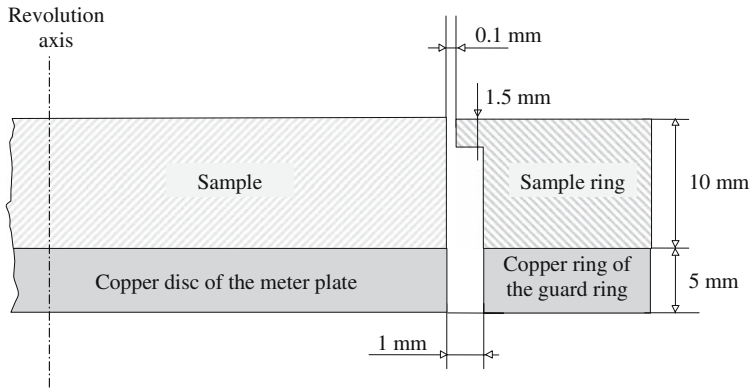


Fig. 3 Expanded view of the gap

2.1 Heating System

Figure 2 shows a cross section of the heating system with the two samples and the thermal guard. For convenience, the following vocabulary, similar to that used by researchers performing thermal-conductivity measurements with guarded hot plates [8,9], is used:

- meter plate: the system used to heat the samples, consisting of an electrical heater (disc) and two copper discs to provide a uniform temperature,
- guard ring: the system used to heat the “sample rings,” consisting of an electrical heater (ring) and two copper rings,
- sample rings: the two rings, heated by the guard ring, that surround the samples.

Two heaters are used, one for the two samples and the other for the two sample rings. The electrical heaters are thin, flexible heating elements consisting of a foil resistive element laminated between layers of polyimide film; the limiting temperature of the heaters is 210°C. The sample heater (disc shape) is sandwiched between two copper discs (diameter = 62.2 mm, thickness = 5 mm), and the guard-ring heater (ring shape) is sandwiched between two copper rings (inner diameter = 64.2 mm, outer diameter = 120.7 mm). The gap between the meter plate and the guard ring (Fig. 3) is 1 mm. On each side of the heating system, the copper disc is attached to the ring by four bindings made of structural epoxy (cross section of 5 mm × 5 mm). The guard-ring temperature is controlled by an eight-stage thermopile across the gap. Four stages of the thermopile are embedded in the copper disc and the copper ring of each side of the heating plate. The thermopile wires are embedded in grooves filled with epoxy resin with “high” thermal conductivity ($1.8 \text{ W} \cdot \text{m}^{-1} \cdot \text{K}^{-1}$). The temperature of the meter plate is controlled by a chromel/alumel thermocouple embedded in one of the two copper discs.

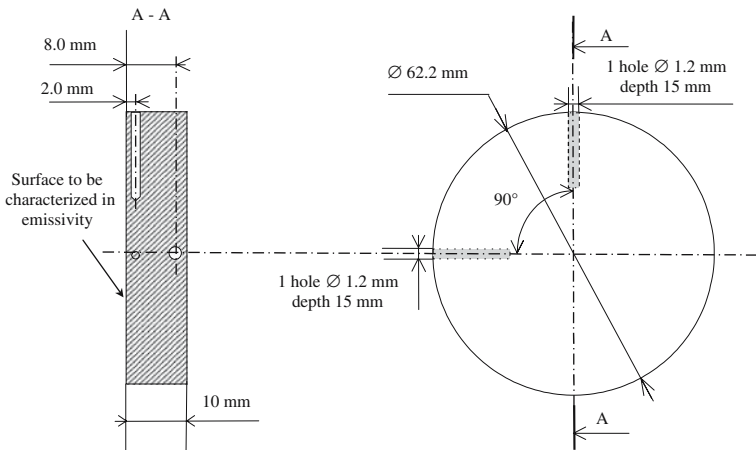


Fig. 4 Samples

2.2 Samples

Two identical samples are needed for a measurement. The shape and dimensions of the samples are shown in Fig. 4. Two radial holes (diameter of 1.2 mm) are drilled in each sample at known distances from the surface. If the material, to be characterized in emissivity, is thin, then two samples of the material are placed on two metallic discs with one or two holes for thermocouples. If the material is a coating (paint, varnish, . . .), then the coating is applied to two metallic discs.

2.3 Sample Rings

Each sample is surrounded by a ring (called “sample ring”) heated by the guard ring. Ideally, the sample rings would be made of the same material as the samples, in order to have the same distribution of temperature as the sample (same gradient). In fact, for convenience, three sets of sample rings can be used, one made of stainless steel, one made of aluminum alloy, and one made of copper. The sample rings are fastened to the guard ring with screws. Three small clamps attached to each sample ring are used to press each sample on the meter plate.

2.4 Wire Guard Block

A thermal guard (called “wire guard block”) is used to heat all the wires that connect the heating system to the measuring devices or the electrical supplies (thermocouples, thermopile, electrical supplies). A similar system is described in Ref. [5] for an emissometer and in Ref. [9] for a guarded hot plate used for thermal-conductivity measurements. The “wire guard block” is used to avoid an important local perturbation of the temperature distribution in the guard ring. The temperature of the

block is controlled by a differential thermocouple between the block and the guard ring.

2.5 Vacuum Chamber

The chamber, made of stainless steel, has an internal surface area of 1.36 m^2 . The surface is coated with Nextel velvet coating 811-21 black paint. The total hemispherical emissivity of the paint, measured by PTB (Physikalisch Technische Bundesanstalt), is 0.943 at -60°C [10]. A well (diameter of 200 mm) is used to insert the heating system inside the chamber. The wall of the well is electro-polished to reduce the emissivity. A stacking of three screens, made of polished aluminum, is used to reduce the direct radiation flux, coming from the upper and hotter part of the well, inside the chamber. The air is pumped out through an opening between the screens and the tube.

2.6 Vacuum Pumping System

The pumping system is made of a turbomolecular pump associated with rotary vane pumps. The gas in the chamber is pumped out, while the chamber is at ambient temperature, until the pressure reaches $5 \times 10^{-3}\text{ Pa}$. Then liquid nitrogen is transferred into the Dewar, and the pressure in the chamber falls to less than 10^{-3} Pa .

2.7 Instrumentation and Control Devices

The temperatures in the heating plate (meter plate and guard ring), in the two samples, and in the sample rings are measured with chromel/alumel thermocouples connected to a high-precision calibrated voltmeter. The temperature of the meter plate and that of the guard ring are controlled by a dual loop Eurotherm controller with high resolution. Each loop of the controller pilots a dc power supply. The intensity supplied to the meter plate is measured indirectly by measuring the voltage at the terminals of a calibrated shunt resistor, and the voltage is measured directly at the terminals of the heater (inside the meter plate). The pressure in the chamber is controlled with a Penning manometer.

3 Measurement Procedure

First, the two samples are characterized geometrically (diameter of the radiating surface, thickness, and positions of the two radial holes). The samples are attached to the heating system with thermal grease applied between the samples and the meter plate to provide good thermal contact; thermal grease is also applied between the sample rings and the guard ring. The thermal grease is used to reduce temperature unbalance between the two samples and between the samples and the rings and to improve the homogeneity of temperature.

The heating system (with the samples and the rings) is suspended at mid-height of the vacuum chamber. The air is pumped out until the pressure is below $5 \times 10^{-3}\text{ Pa}$.

The Dewar is filled until the level of liquid nitrogen is 5 cm higher than the top of the vacuum chamber. The temperatures of the heating system (meter plate and guard ring) are stabilized at the required level; the time to reach good stability is about 4 h.

The temperatures of the two samples and the two sample rings are measured to ensure that the two samples and the two rings are at approximately the same temperature. The temperatures in the two samples and the two rings are measured along with the electrical power supplied to the meter plate. These measurements are repeated at least 30 times, and the mean emissivity is calculated.

4 Emissivity Calculations

4.1 Emissivity Calculations

The total hemispherical emissivity is computed from the net heat-transfer rate of the circular surfaces of the samples. Many models, more or less complex, can be developed to relate the emissivity to the electrical power supplied to the meter plate, to the surface temperature of the samples, and to the temperatures of the surfaces present in the surroundings of the samples. The complexity of the model depends on the number of surfaces that are considered. Most of the models found in the literature are very simple; for example, the emissivity of the chamber walls is considered to be one, as in Refs. [6] and [11], or the number of elements is reduced to the samples and the chamber walls [5].

Our model considers three surfaces: the circular radiating surfaces of the two samples, the surfaces of the rings (plane annular surfaces and cylindrical surfaces), and the chamber walls. The model is developed using the radiosity method, that is to say, by considering that the emissions of the surfaces are Lambertian, the reflections on the surfaces are perfectly diffuse, and the spectral emissivities of the surfaces are independent of wavelength.

The heat balance equation for the two samples gives the relation,

$$\varepsilon_s = \frac{\frac{(P_{\text{elec.}} - P_{\text{leaks}})}{S_s} \left(\varepsilon_c + \varepsilon_r \frac{S_r}{S_c} (1 - \varepsilon_c) \right)}{\sigma T_s^4 \left(\varepsilon_c + \varepsilon_r \frac{S_r}{S_c} (1 - \varepsilon_c) \right) - \varepsilon_c \sigma T_c^4 - (1 - \varepsilon_c) \left(\varepsilon_r \frac{S_r}{S_c} \sigma T_r^4 + \frac{(P_{\text{elec.}} - P_{\text{leaks}})}{S_c} \right)} \quad (1)$$

where ε_s is the total hemispherical emissivity of the samples, $P_{\text{elec.}}$ is the electrical power supplied to the meter plate, P_{leaks} is the thermal power “lost” by the samples and the meter plate by ways other than radiation by the two circular surfaces of the samples, S_s is the sum of the two circular surface areas of the samples, ε_c is the total hemispherical emissivity of the chamber walls, ε_r is the mean total hemispherical emissivity of the surfaces of the rings, S_r is the surface area of the sample rings radiating toward the chamber walls, S_c is the surface area of the chamber walls, σ is the Stefan–Boltzman constant, T_s is the mean surface temperature of the two samples, T_c is the mean temperature of the chamber walls, and T_r is the mean surface temperature of the two rings. P_{leaks} is considered positive when heat is lost by the samples or by the meter plate and is considered negative when heat is gained.

The real surface temperatures of the two samples are slightly different; thus, the mean surface temperature used to calculate the emissivity is calculated using the relation,

$$T_s = \left(\frac{S_{s1} T_{s1}^4 + S_{s2} T_{s2}^4}{S_{s1} + S_{s1}} \right)^{\frac{1}{4}} \quad (2)$$

where T_s is the mean surface temperature of the two samples, S_{s1} is the area of the circular surface of sample No. 1, S_{s2} is the area of the circular surface of sample No. 2, T_{s1} is the surface temperature measured for sample No. 1, and T_{s2} is the surface temperature measured for sample No. 2.

4.2 Uncertainty of the Model

The uncertainty of the model has been evaluated by comparison to a model considering five surfaces. The “true” value of the power radiated by the samples is assumed to be the one given by the five-surface model (chamber walls, samples, guard rings, screens, and opening of the well). The relative difference between the emissivity calculated with the three-surface model and the “true” emissivity is less than 0.11%.

4.3 Heat Loss Evaluation

The unwanted heat fluxes lost or gained by the samples and the meter plate are:

- the radiation flux by the edge of the samples (cylindrical surface),
- the radiation flux by the edge of the meter plate (copper discs),
- the conduction flux between each sample and the sample ring, and
- the flux lost by conduction or convection though the air remaining in the chamber.

4.3.1 Edge Losses by Radiation

The geometry of the gap is shown in Fig. 3. A radiosity model was developed to calculate the radiative net heat flux lost by the sample edge (cylindrical surface). Due to the symmetry of the system, the calculation was done only for one side of the heating system. In the model each surface is assumed to be isothermal. So the calculation was done considering the mean temperature of the sample and of the sample ring. The results show that, if the mean temperature of the sample is the same as that of the sample ring, the gap radiates toward the chamber like a blackbody at the mean temperature of the sample. This is not surprising because of the low value of the ratio of the surface area of the opening of the gap to the internal surface area. Thus, if the mean temperature of the sample is the same as that of the sample ring, the heat flux lost by radiation by the edge of the sample depends almost completely on the ratio of the emissivity of the sample edge to the emissivity of the edge of the sample ring; Fig. 5 shows that evolution. If the heating system is isothermal and if the emissivity of

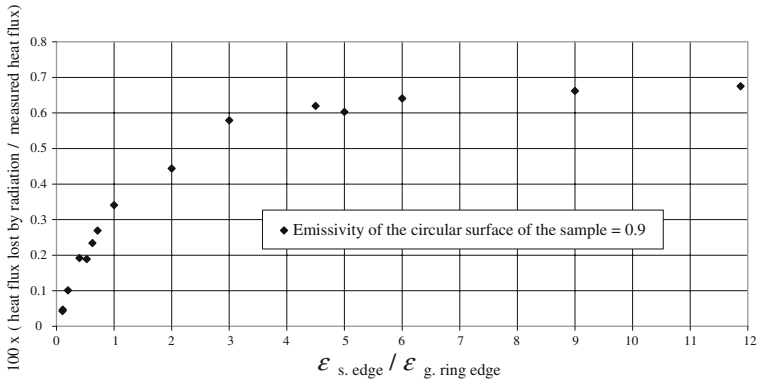


Fig. 5 Radiative heat flux lost by the edge of the sample: $\epsilon_{s, \text{edge}}$ is the emissivity of the edge of the samples, and $\epsilon_{g, \text{ring edge}}$ is the emissivity of the edge of the guard rings

the sample edge is the same as that of the edge of the ring, then the heat flux lost by radiation by the sample edge is equivalent to an emissivity of 0.0032 for the circular surfaces of the samples. The heat flux, lost or gained by the edges of the samples, is calculated for each material and the related correction is applied to the measured emissivity. If the emissivity of the edges of the samples is approximated, then the uncertainty of the correction is quantified by varying the value of the emissivity of the edges.

4.3.2 Edge Losses by Conduction

A difference of temperature between each sample and the corresponding sample ring can occur if the thermal contact resistance between the sample ring and the guard ring is different from that between the sample and the meter plate. The temperature of each ring is measured using two thermocouples, just as for the samples. The value evaluated for the heat transfer coefficient by conduction through the four thermocouples embedded in the samples is $0.074 \text{ W} \cdot \text{K}^{-1}$.

The heat flux by conduction between the meter plate and the guard ring is assumed to be negligible because the temperature of the guard ring is controlled to be almost the same as that of the meter plate. Nevertheless, a contribution to the uncertainty is considered for that heat flux.

4.3.3 Heat Loss by the Air Remaining in the Chamber

During emissivity measurements the air remaining in the chamber is at a pressure below 10^{-3} Pa . The longer distance between the samples and a point of the chamber walls is about 300 mm. At a pressure below 10^{-3} Pa , the mean free path for a molecule of air is larger than 1 m [12], that is, the mean free path is larger than the greatest dimension of the chamber. The heat flux lost by the circular surface of a sample is

Table 1 Power supplied to the meter plate versus pressure and heat transfer coefficient through the air

Pressure (Pa)	Measured power (W)	Heat transfer coefficient through the air (W · m ⁻² · K ⁻¹)	Heat transfer coefficient cal- culated using Eq. 4 (W · m ⁻² · K ⁻¹)
2.00 × 10 ⁻⁴	0.366	4.4 × 10 ⁻⁴	2.4 × 10 ⁻⁴
5.00 × 10 ⁻⁴	0.367	1.0 × 10 ⁻³	6.0 × 10 ⁻⁴
2.00 × 10 ⁻³	0.370	2.7 × 10 ⁻³	2.4 × 10 ⁻³
5.00 × 10 ⁻³	0.375	5.4 × 10 ⁻³	6.0 × 10 ⁻³
2.00 × 10 ⁻²	0.406	2.3 × 10 ⁻²	—
5.00 × 10 ⁻²	0.435	3.9 × 10 ⁻²	—
2.00 × 10 ⁻¹	0.491	7.0 × 10 ⁻²	—

given by the following relation [13]:

$$\Phi_{\text{air}} = S_{\text{samples}} a \frac{\gamma + 1}{2(\gamma - 1)} \sqrt{\frac{R}{2\pi MT}} p (T_{\text{sample}} - T_{\text{walls}}) \quad (3)$$

where S_{samples} is the surface area of the sample, a is the accommodation coefficient ($a = 1$ for air at 77.4 K [13]), γ is the ratio of the heat capacities of the air ($\gamma = 1.40$ for air [14]), R is the universal gas constant ($8.314 \text{ J} \cdot \text{mol}^{-1} \cdot \text{K}^{-1}$ [14]), M is the molar mass of air (28.97 g [14]), T is the temperature of the manometer (293 K), p is the pressure of the air, T_{sample} is the surface temperature of the sample, and T_{walls} is the temperature of the chamber walls. The relation becomes

$$\Phi_{\text{air}} = S_{\text{samples}} K p (T_{\text{sample}} - T_{\text{walls}}) \quad (4)$$

with $K = 1.2 \text{ W} \cdot \text{m}^{-2} \cdot \text{Pa}^{-1} \cdot \text{K}^{-1}$.

Measurements of variations of the power supplied to the meter plate versus pressure in the chamber were made; the results are given in Table 1. The measurements were made with low emissivity samples ($\varepsilon = 0.055$) at 100°C. The power varies linearly with the pressure for a pressure below $2 \times 10^{-2} \text{ Pa}$ (molecular regime). The experimental heat transfer coefficient was calculated considering that the power for the perfect vacuum can be calculated by linear extrapolation from the powers measured at low pressures. The theoretical heat transfer coefficient given by Eq. 4 is also given in Table 1. The measured heat transfer coefficient is of the same order as that given by theory for a pressure below $5 \times 10^{-3} \text{ Pa}$. Table 2 gives, for different temperatures, the emissivity equivalent to the power lost through the air. A reasonably good vacuum is needed to have a low error; a pressure lower than 10^{-3} Pa results in a low error over the complete temperature range.

Table 2 Emissivity equivalent to the heat loss through the air

Pressure (Pa)	Emissivity equivalent to the heat loss through the air			
	Surface temperature			
	−20°C	20°C	100°C	200°C
1.0×10^{-4}	0.0001	0.0001	0.0000	0.0000
5.0×10^{-4}	0.0005	0.0003	0.0002	0.0001
1.0×10^{-3}	0.0009	0.0006	0.0003	0.0002
5.0×10^{-3}	0.0046	0.0031	0.0016	0.0008

5 Assessment of Uncertainties

The method used to calculate the uncertainty is the one recommended by the International Committee for Weights and Measures (CIPM) in the Guide to the Expression of Uncertainty in Measurement [15]. Equation 1 is used to calculate the mean emissivity of the two samples. The uncertainty in the emissivity due to each input parameter is calculated considering the uncertainty of the input and the sensitivity coefficient of the emissivity with the input parameter. Two other sources of uncertainty are considered: the model used to calculate the emissivity (Eq. 1) and the random variations of the input parameters during a series of measurements. The experimental standard deviation of a series of emissivity results integrates the random variations of all the input parameters that can vary during a series of measurements (temperatures, electrical power, heat fluxes). The uncertainty related to the model has been quantified by comparison to a less simplified model supposed to be more realistic (see Section 4.2). Table 3 gives a list of the uncertainty sources that are considered. The numerical values in Table 3 were evaluated for the particular case of a black paint (thickness = 50 μm) applied on copper substrates; the samples were at 20°C and the measured total hemispherical emissivity was 0.921. All uncertainties given in the table are expanded uncertainties with a coverage factor $k = 2$.

6 Validation of Measurements

The measurement technique was validated by comparison with a radiative technique used at Physikalisch Technische Bundesanstalt (PTB) in Germany [1]. PTB measured the total directional emissivity, for many directions between 0° and 75° (angle to the normal), by comparison to a blackbody with a total (same sensitivity for all wavelengths) radiometer. A model of angular variation was then applied, and the hemispherical total emissivity was calculated by integration over the half-space.

The material selected for the comparison was AISI 304 L stainless steel. The samples were sandblasted and oxidized by heating in air at 360°C. The results are given in Table 4. For LNE, the results are the mean emissivities of the two samples. For PTB, the emissivity given for 40°C is that measured on sample No. 1. For 150 and 200°C, the values are the means of the emissivities measured independently on the two samples. For 150 and 200°C, the differences between the emissivities of the two samples, measured by PTB, are less than 0.006. The results of the two laboratories are

Table 3 Budget of uncertainty for a black paint at 20°C

Parameter or model	Value & expanded uncertainty ($k = 2$)	Estimated uncertainty in the measured emissivity ($k = 2$)	expanded in the emissivity
Surface area of the samples	$0.006077 \pm 4 \times 10^{-6} \text{ m}^2$	6.1×10^{-4}	
Surface area of the chamber	$1.36 \pm 0.1 \text{ m}^2$	3.3×10^{-4}	
Surface area of the sample rings	$0.0240 \pm 0.0008 \text{ m}^2$	4×10^{-5}	
Mean total hemispherical emissivity of the chamber walls	0.92 ± 0.05	1.3×10^{-3}	
Mean total hemispherical emissivity of the rings	0.8 ± 0.1	1.7×10^{-4}	
Electrical power	$2.38950 \pm 7 \times 10^{-5} \text{ W}$	2.8×10^{-5}	
Mean surface temperature of the sam- ples	$293.5 \pm 0.2 \text{ K}$	2.5×10^{-3}	
Mean temperature of the chamber walls	$77.4 \pm 2 \text{ K}$	5×10^{-4}	
Mean surface temperature of the rings	$293.0 \pm 0.2 \text{ K}$	4×10^{-6}	
Edge heat loss by radiation	$0.0076 \pm 0.002 \text{ W}$	8×10^{-4}	
Edge heat loss by conduction between the samples and the rings	$0.0325 \pm 0.01 \text{ W}$	4×10^{-3}	
Edge heat loss by conduction between the meter plate and the guard ring	$0 \pm 0.006 \text{ W}$	2.4×10^{-3}	
Heat loss by air	$0.0016 \pm 0.0005 \text{ W}$	2×10^{-4}	
Model used for emissivity calculation	± 0.001	1×10^{-3}	
Random variations of measured emis- sivities ($2 \times$ experimental standard deviation)	± 0.002	2×10^{-3}	
Measured emissivity	0.921	0.0061	

Table 4 Comparison of the results of PTB and LNE

Température	Total hemispherical emissivity (oxidized AISI 304L stainless steel)		
	LNE	PTB	PTB–LNE
40°C	0.399 ± 0.0060	0.420 ± 0.04	0.021
150°C	0.427 ± 0.0068	0.433 ± 0.02	0.006
200°C	0.441 ± 0.0075	0.438 ± 0.02	-0.003

in agreement within the combined uncertainties. The uncertainties of LNE are much less than those of PTB, probably because the method of measurement is more direct and requires fewer parameters to be measured (directional emissivity for PTB). For the temperature 40°C, the uncertainty of PTB is large because the radiative emission of the sample is low.

7 Conclusions

LNE has developed an apparatus for measuring the total hemispherical emissivity of solid opaque materials. The emissivity can be measured in the temperature range from -20 to 200°C , on materials with a thermal conductivity higher than $0.2 \text{ W} \cdot \text{m}^{-1} \cdot \text{K}^{-1}$. The sources of errors and the sources of uncertainties have been analyzed in detail. The parasitic heat fluxes at the edge of the samples are not negligible and corrections must be applied to the measured electrical power.

The main sources of uncertainty are:

- uncertainty in the heat flux between the samples and the rings, due to the uncertainty in the difference of temperature between the samples and the rings,
- uncertainty in the surface temperatures of the samples which depends on the thermal conductivity of the material, the level of temperature, and the emissivity of the surface,
- uncertainty in the heat flux between the meter plate and the guard ring.

The targets of uncertainty are reached; the expanded uncertainties ($k = 2$) are less than: ± 0.01 for a material with a thermal conductivity higher than $10 \text{ W} \cdot \text{m}^{-1} \cdot \text{K}^{-1}$ independent of the emissivity, ± 0.01 for a material with an emissivity lower than 0.1 and a thermal conductivity higher than $0.2 \text{ W} \cdot \text{m}^{-1} \cdot \text{K}^{-1}$, and ± 0.03 for a material with a thermal conductivity higher than $0.5 \text{ W} \cdot \text{m}^{-1} \cdot \text{K}^{-1}$ and a high emissivity. Those levels of uncertainty are satisfactory for most applications of heat balance calculations (industrial processes, thermal isolation of buildings, etc.).

References

1. J. Lohrengel, *Wärme Stoffübertrag.* **21**, 1 (1987)
2. J. Hladik, in *Métrologie des Propriétés Thermophysiques des Matériaux* (Masson, Paris, 1990), pp. 271–274.
3. K. Maglic, A. Cezairliyan, V. Peletsky, in *Compendium of Thermophysical Property Measurements Methods—1 Survey of Measurement Techniques* (Plenum Press, New York, 1974), pp. 750–754
4. S. Cheng, P. Cebe, L. Hanssen, D. Riffe, A. Sievers, *J. Opt. Soc. Am.* **4**, 351 (1987)
5. M.C. Certiat, O. Mace, Caractérisation expérimentale de l'émissivité: Besoins pour Aérospatiale, Méthodes développées. Société Française des Thermiciens, Section Rayonnement, Journée d'étude du 17 Avril 1991 sur Pyrométrie Optique, Mesures des émissivités (1991)
6. K. Fukuzawa, A. Ohnishi, Y. Nagasaka, *Int. J. Thermophys.* **23**, 319 (2002)
7. D. Naws, B. Pouilloux, *High Temp. Chem. Processes.* **3**, 99 (1994)
8. Thermal Insulation—Determination of Steady-State Thermal Resistance and Related Properties—Guarded Hot Plate Apparatus, ISO 8302. Int. Org. Standardization, Geneva, Switzerland (1991)
9. R.R. Zarr, W. Healy, J.J. Filliben, D.R. Flynn, Design Concepts for a New Guarded Hot Plate Apparatus for Use Over an Extended Temperature Range. Reprinted from STP 1426, ASTM International Standards, Insulation Materials, Testing and Applications, V4-ISBN 0-8031-2898-3 (2002)
10. J. Lorengel, R. Todtenhaupt, in *Wärmeleitfähigkeit, Gesamtemissionsgrade und spektrale Emissionsgrade der Beschichtung Nextel-Velvet Coating 811-21*. PTB-Mitteilungen 106 4 (1996)
11. Y.S. Touloukian, D.P. DeWitt, in *Thermophysical Properties of Matter*, vol. 7 (IFI/Plenum, New York, Washington, 1970), pp. 40a–42a
12. G. Rommel, *Gaz à très basse pression—Généralités, Ref B4020* (Techniques de l'Ingénieur, Paris, 1984)
13. A. Bui, B. Hébral, F. Kircher, Y. Laumond, Locatelli, M., Verdier, J.: *Cryogénie: propriétés physiques aux basses températures, Ref B2380* (Techniques de l'Ingénieur, Paris, 1993)

14. R. Gicquel, *Diagrammes thermodynamiques, Ref BE8040* (Techniques de l'Ingénieur, Paris, 2002)
15. Guide to the Expression of Uncertainty in Measurement (International Organisation for Standardisation, Geneva, Switzerland, 1995)